Science of the Total Environment xxx (xxxx) xxx

Contents lists available at ScienceDirect

Science of the Total Environment

journal homepage: www.elsevier.com/locate/scitotenv

Formation of cluster mode particles (1–3 nm) in preschools

Mehdi Amouei Torkmahalleh [a,*], Kamila Turganova [a], Zhuldyz Zhigulina [a], Tomiris Madiyarova [a], Enoch Kwasi Adotey [a], Milad Malekipirbazari [b], Giorgio Buonanno [c], Luca Stabile [c]

[a] Department of Chemical and Materials Engineering, School of Engineering and Digital Sciences, Nazarbayev University, Nur-Sultan 010000, Kazakhstan
[b] Department of Industrial Engineering, Bilkent University, 06800 Bilkent, Ankara, Turkey
[c] Department of Civil and Mechanical Engineering, University of Cassino and Southern Lazio, via Di Biasio 43, Cassino 03043, Italy

HIGHLIGHTS

- Cluster mode particles (1–3 nm) were observed in preschools.
- Candle burning produces primary cluster mode particles.
- Indoor VOCs are the controlling factors in production of cluster mode particles.
- Emission rate of the particles varies with the type of the cleaning products.
- Opportunities exits to reduce exposure to particles in preschools.

GRAPHICAL ABSTRACT

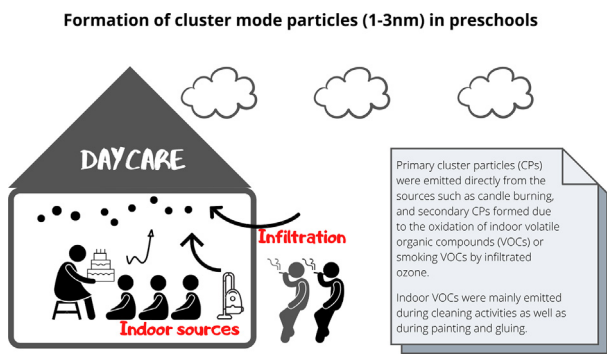

ARTICLE INFO

Article history:
Received 22 April 2021
Received in revised form 11 November 2021
Accepted 13 November 2021
Available online xxxx

Editor: Jianmin Chen

Keywords:
Cluster mode particles
Preschool
Cleaning detergents
SOA
Ozone

ABSTRACT

This study is the first study that reports the cluster particle (1–3 nm) formation (CPF) in two modern preschools located in Nur-Sultan city of Kazakhstan from October 28 to November 27, 2019. The average particle number concentration and mode diameter values during major CPF events in Preschool I and Preschool II were found to be 1.90×10^6 (SD 6.43×10^6) particles/cm^3 and 1.60 (SD 0.85) nm, and 1.11×10^9 (SD 5.46×10^9) particles/cm^3 and 2.16 (SD 1.47) nm, respectively. The ultraviolet PM concentration reached as high as 7 μg/m^3 in one of the measurement days. The estimated emission rate in Preschool I for CPF events was 9.57×10^9 (SD 1.92×10^9) particles/min. For Preschool II, the emission rate was 7.25×10^9 (SD 12.4×10^9) particles/min. We identified primary cluster particles (CPs) emitted directly from the sources such as candle burning, and secondary CPs formed as a result of the oxidation of indoor VOCs or smoking VOCs. The secondary CPs are likely to be SOA. Indoor VOCs were mainly emitted during cleaning activities as well as during painting and gluing. Indoor VOCs are the controlling factors in the CPF events. Changes in the training and cleaning programs may result in significant reductions in the exposure of the children to CPs.

1. Introduction

Ultrafine particles (particles with an aerodynamic diameter smaller than 100 nm) in great quantities are hazardous for pulmonary and extra-pulmonary systems such as the heart and brain through inhalation (Oberdörster et al., 2004; Slezakova et al., 2019; Rim et al., 2017; Naseri et al., 2019). Although studies show that these small particles contribute very little to the overall mass of particles, they cause a greater adverse impact on human (Fonseca et al., 2014; Morawska et al., 2008).

* Corresponding author.
E-mail address: mehdi.torkmahalleh@nu.edu.kz (M. Amouei Torkmahalleh).

http://dx.doi.org/10.1016/j.scitotenv.2021.151756

Exposure to ultrafine particles (UFPs) was investigated at homes, schools, offices and aged care facilities (Morawska et al., 2017a), and their primary sources were identified and discussed. Moreover, a secondary formation of UFP appears to be a significant source of secondary organic aerosol (SOA) as a result of the reaction between O_3 and volatile organic (Slezakova et al., 2019; Sarwar et al., 2003a). However, less attention was made to study the exposure of preschool children to UFPs, particularly SOA.

In preschools, children spend up to 7 h per day, and therefore, it is important to estimate the particle concentrations in the preschools due to their immature respiratory systems. Preschool children are exceptionally vulnerable to diseases caused by inhaling air pollutants. (Oliveira et al., 2017) Moreover, due to the more frequent inhalation rate, children breathe in more PM mass concentration per weight in comparison to adults (Gaspar et al., 2018).

Several studies examined the air quality in schools in different countries (Daisey et al., 2003; Ramachandran et al., 2005; Godwin and Batterman, 2007). Chithra and Nagendra (2012) investigated the air quality in 8 schools in Chennai, India. PM analysis data indicated that the measured values often exceeded the guidelines proposed by the National Ambient Air Quality Standards. Indoor-to-outdoor (I/O) ratios were always higher than 1, suggesting that the source of PM inside the classrooms were indoor activities of occupants. Sohn et al. (Yang et al., 2009) monitored the air quality in three different school buildings in Korea, including the measurements of PMs, CO and CO_2 gases, and VOCs. The concentration of PM_{10} in classrooms was the highest compared to the laboratories and computer rooms by less than 50%, while the concentration of CO_2 and VOCs in the classrooms were three to four times higher than those in the laboratories and computer rooms, suggesting that the main source of the pollutants were indoor activities and consequent particle resuspension. It was also proposed that poor ventilation causes the higher PM values. Independent studies in Portugal, Central Europe, and Turkey in elementary schools and preschools found that the detected indoor concentrations of VOCs were several times higher than that outdoors, suggesting that the source of VOC was present indoors (Pegas et al., 2010; Kotzias, 2005; Sofuoglu et al., 2011). Pegas et al. (2010) in their study discovered that when glue and paints were used in the class, VOC concentrations increased significantly.

Amouei Torkmahalleh et al. (2021) summarized some key findings about indoor air quality in preschools. Morawska et al. (Morawska et al., 2017b) studied the exposure of preschool children to PM_{10}, $PM_{2.5}$, and particle number concentrations. They found that average $PM_{2.5}$ concentration inside the preschools was 52.3 μg/m^3 (comparing to the outdoor 7.60 μg/m^3), for the occupancy period and indicated that indoor sources were the primary source of the particles. In Poland, Błaszczyk et al. (2017) investigated air quality in rural and urban preschools. They found that average $PM_{2.5}$ concentrations within preschools ranged from 18.5 to 42.4 g/m^3 for urban preschools and from 20.0 to 41.9 g/m^3 for rural preschools, respectively. Coal and wood burning in residential stoves used for heating in cold seasons were discovered to be a source of indoor pollutants.

SOA can also contribute considerably to UFP concentration indoors. Pioneers in indoor SOA observation were Wechsler and Shields (Weschler and Shields, 1999), who stated the mechanism of SOA formation as a result of ozone and indoor gas (D-limonene) reaction. The chemistry of "terpenoids" indoor gas group ozonolysis was found to result in SOA formation (Bahreini et al., 2005; Chen and Hopke, 2010; Sarwar et al., 2003b; Waring et al., 2011; Coleman et al., 2008; Destaillats et al., 2006; Donahue et al., 2007; Fadeyi et al., 2013; Leungsakul et al., 2005; Librando and Tringali, 2005; Presto et al., 2005; Sarwar and Corsi, 2007). Terpenoids can be presented by various gases such as D-limonene (Błaszczyk et al., 2017; Sarwar et al., 2003b; Waring et al., 2011; Coleman et al., 2008; Destaillats et al., 2006), monoterpenes (Donahue et al., 2007; Fadeyi et al., 2013; Leungsakul et al., 2005) and terpene mixture (Librando and Tringali, 2005). Although ozone concentration is determined by the outdoor conditions, Terpenoids can be produced by the indoor consumer products and cleaning products (Kotzias, 2005; Sofuoglu et al., 2011; Presto et al., 2005; Sarwar and Corsi, 2007). Ones originated from detergents are claimed to be one of the major indoor SOA source (Waring and Siegel, 2013; Walser et al., 2007), which can be detrimental for the human health (Rohr, 2013; Kephalopoulos et al., 2007).

Study of Morawska et al. (2009) observed SOA formation in the Australian school. It was found out that monoterpene from the detergent product was a source of SOA formation, which vastly contributed to ultrafine particles concentration indoors. Moreover, it was highlighted that most of the SOA precursors were found within the primary school classrooms, owing to the liquid materials presence used for both cleaning and art classes. The case was identified to have a wider scope, since most of preschools and primary schools use liquids (e.g. glue, paintings) for art activities, and detergent (Stabile et al., 2021) are used for cleaning at most types of the educational organizations.

So far, most of the previous studies on indoor UFPs reported particle number concentrations down to 6 nm (Bhangar et al., 2016; Mullen et al., 2011). However, source-specific studies were conducted to examine the size distributions of particles below 3 nm referred to as cluster mode particles. Such studies reported the production of a copious amount of UFPs from candle burning (2.3–64 nm) (Wallace et al., 2019), gas stove particles (2.5–20 nm) (Pedata et al., 2016), stir-frying and cleaning (1 nm-20 μm) (Patel et al., 2020), and peeled orange (1–4 nm) (Wu et al., 2019). New particle formation in the range of 1–3 nm is referred to as "cluster mode" particle formation. This mode of particles was reported in urban environments (Yao et al., 2018), and then efforts were shown to investigate new particles in indoor environments. Ahonen et al. (2017) reported new particle formation between 1 and 2 nm in cleanrooms to be up to 10^5 particles/cm^3 while the sub 7 nm particles were in the order of 10^4 particles/cm^{3,} suggesting the formation of new particles indoors in the absence of human activities. Vanhanen et al. (2016) constantly observed particles/clusters in the size range of 1.15–1.54 nm up to 5×10^3 particles/cm^3 in a laboratory without significant emissions. In a very recent study, Wu et al. (Wu et al., 2019) presented temporal trends in the concentration and size distribution of cluster mode particles down to 1 nm in an office with a HVAC system. They reported peeling mandarins to be a strong source of cluster mode particle formation in the range of 1.4 nm. Patel et al. (2020) observed the formation of 1–3 nm particles in range of 10^6 particles/cm^3 with the mode size of 1.6 nm during different cooking activities. The major source of new particles was concluded to be ozonolysis of monoterpenes in the office. Nevertheless, further investigations are required to understand the major sources of cluster mode particles indoor (primary vs. secondary sources). No study so far demonstrated the source of new particles (1–3 nm) in preschools.

This study aimed to investigate the formation of the cluster mode particles and their emission rates in two preschools (Preschool I and Preschool II) in Nur-Sultan (Astana), the capital of Kazakhstan, and also to identify the potential sources of such particles in the preschools. In Preschool I, the choices of the activities were typically made by the children based on their interests. While, in Preschool II, predefined programs were practiced by the mentors. Thus, two different approaches were practiced in the two preschools that could result in different source and exposure profiles.

2. Methodology

2.1. Sampling sites

Two preschools located in a residential building (20 m away from each other) in Nur-Sultan, the capital of Kazakhstan, were chosen. The preschools opened to the residential building. Preschool I had three classrooms with some windows that could open to the outside as needed. However, during the sampling period, given the low outside temperature, the windows were closed. Preschool II had two classrooms with a connecting hall between them. None of the windows at Preschool II could open to the outside. There was only a small backroom in Preschool II connected to the classroom where the measurements took place. The backroom could be opened to the outside as needed. The children at Preschool II were taken out occasionally in the afternoon through the back room. The door to the outside was not tightly closed, and therefore, there was an opportunity

for particles to penetrate inside. There was air conditioning in the small back room to adjust the indoor temperature.

On the west side of the residential building, a highway with mild traffic existed. Also, an open space parking lot was located on the west side of the building. The highway and the parking lot were closer to Preschool I compared to Preschool II. A dedicated smoking zone existed on the north side of Preschool II at 5 m distance from the back door of Preschool II. People residing in the residential building, as well as the surrounding buildings, frequently smoked during the sampling period from morning till the evening time. This smoking zone was occupied frequently by approximately 5 to 6 persons per half an hour.

A combustion unit was located approximately 1 km away at the north side of the two preschools to provide heating for several commercial sectors near the preschools. Fig. S1 shows the locations of the two preschools, the highway, and the parking lot.

The measurements in Preschool I were conducted from October 28 to November 1, 2019 and November 16 and 17, 2019 (for background measurements). In total, five days of weekdays and two days of a weekend (for the background measurements) were spent for the experiments. In Preschool II, monitoring was performed for 9 days from November 18 to November 27, 2019 including Sunday, November 24, 2019 (for the background measurement).

2.1.1. Preschool I

The sampling was conducted in a classroom where a higher population of children were present, and the children spent most of their time in that room. The volume of the room in preschool I was approximately 30.6 m^3. There were two windows in the room. Typically, daily activities included playing, dancing, drawing, eating breakfast and lunch, microwaving, cleaning the floor using a vacuum cleaner, dust cleaning from tables and chairs, etc. Briefly, in Preschool I, during the morning, the children played with cards and pieces, did gluing, painting, etc. and before noon, they danced with music and blew off some candles. During noontime, the children left the preschool facility to a nearby gym. Approximately at 1 pm, they returned to the preschool and ate their lunch meals which were already heated in the microwave by the mentors. In the afternoon, the kids again played games, and occasionally the birthday cake was served, and birthday candles were blown off. Children in the range of 2 to 6 years old were admitted to Preschool I. The approximate total number of people in the room, including kids and mentors, was 18. The measurements were conducted during the working hours from 9:30 am, when children usually came to the preschool, to 4:00 pm, when children left the facility. Fig. S2 shows the location of the instruments inside Preschool I.

2.1.2. Preschool II

The detailed information about Preschool II is found in the supplementary materials.

2.2. Measurements and instrumentation

2.2.1. Indoor monitoring

The instruments inside the classroom were placed about 1 m away from the window and about 1 m high from the floor, at the breathing zone of the children. Figs. S2 and S3 show the indoor sampling locations in Preschools I and II, respectively.

2.2.1.1. Preschool I. Indoor temperature, RH, CO, and CO_2 were monitored using IAQ-Calc™ Indoor Air Quality Meter (Model 7545, TSI, USA) with one-minute logging intervals. A Scanning Mobility Particle Sizer (SMPS) (Model 8533, TSI, USA) was utilized in this study to investigate the particle number size distribution. The SMPS was equipped with a Nano (short) DMA. The reading intervals of SMPS were 75 s, including 60s scan time and 15 s for purging. The maximum total particle concentration detectable by SMPS was 10^7 particles/cm^3, according to the manual of the instrument. When the short DMA was used, the size range of the SMPS was adjusted from 1 nm to 10 nm. A Condensation Particle Counter (CPC) (Model 3007, TSI, USA) with 1 min logging interval was used in this study to count the particles larger than 10 nm. In this case, total particle number concentrations from 1 nm to the upper size of CPC were estimated. The CPC measures the total particle number concentration up to 10^5 particles/cm^3. However, for concentrations larger than this value shown by the CPC, a correction equation was applied (Eq. (1)).

$$y = 6 \times 10^{-19}x^4 - 10^{-12}x^3 - 4 \times 10^{-8}x^2 + 0.9x + 9660.1 \quad (1)$$

where x is the cpc measured concentration above 1.00×10^5 particles/cm^3, and y is the corrected concentration (particles/cm^3).

2.2.1.2. Preschool II. Supplementary material presents the measurements and instrumentation regarding Preschool II.

2.2.2. Outdoor monitoring

2.2.2.1. Preschool I. An integrated air quality monitoring station (Model AQS1, Aeroqual, New Zealand) was installed at the west side of Preschool I, 2 m away from its window, to monitor nitrogen dioxide (NO_2) and ozone (O_3) concentrations. Meteorological data, including wind speed, wind direction, outdoor temperature, and RH were recorded by AQS1 and were accessible with 1 min logging intervals through a cloud system. The recommended operating temperature by the manufacturer of the AQS1 was −10 °C. However, during the monitoring period in Preschool I, the outdoor temperature in Nur-Sultan was higher than −10 °C.

2.2.2.2. Preschool II. The detailed information about Preschool II is found in the supplementary materials.

2.3. Cluster particle formation (CPF)

In this study, a CPF event refers to when particles smaller than 3 nm are produced. However, if the concentrations of the sub-3 nm particles are above 10^6 particles/cm^3 it is considered a major CPF event. If the concentration is less than 10^6 particles/cm^3, it is considered a minor CPF event.

2.4. Indoor air exchange rate and emission rate calculation

The air exchange rate was calculated using the CO_2 decay period with the following equation:

$$\mathrm{Ln}\frac{(C_{in,t} - C_{in,b})}{(C_{in,max} - C_{in,b})} = -\mathrm{AER}*t \quad (2)$$

where AER (air exchange rate) is the negative slope obtained from the graph of $\mathrm{Ln}\frac{(C_{in,t}-C_{in,b})}{(C_{in,max}-C_{in,b})}$ versus time (in min).

C_{in} and $C_{in,0}$ represent the peak and initial (background) indoor CO_2 concentrations, respectively, and t is the time difference between initial and peak concentrations. AER is the air exchange rate (as obtained through the CO_2 decay test).

Emission rate was calculated using the following formula, which was applied in several papers for calculating emissions rates for different indoor sources (Amouei Torkmahalleh et al., 2018; Wallace et al., 2004):

$$\mathrm{Ln}\Delta C = \mathrm{Ln}\frac{S}{V(a+k)} + \mathrm{Ln}[1 - \exp(-(a+k)t)] \quad (3)$$

where ΔC represents the difference of the measured indoor and background concentrations, (a + k) is the decay rate, calculated from the Eq. (4).

$$\mathrm{Ln}\frac{(C_{in,t} - C_{in,b})}{(C_{in,max} - C_{in,b})} = -(a+k) * t \quad (4)$$

C_{in} and $C_{in,0}$ represent the peak and initial (background) indoor particle concentrations, respectively.

The y-intercept of the graph LnΔC versus Ln[1 − exp (−(a + k)t)] is Ln $\frac{S}{V(a+k)}$. Value of S, emission rate, is calculated. Eq. (3) is a simplified form of the mass-balance equation and assumes a constant emission rate, removal rate, and air exchange rate over the time of Δt. Furthermore, Eq. (3) ignores the coagulation of the particles, and thus, the estimated emission rate is considered as the lower limit of the emission rate in the preschools. The emission rate was estimated for the size range of 1–30 nm.

3. Results

In this section, the particle number concentration values shown by the counter plots were created using SMPS data. The figures presenting total particle number concentrations were plotted using both CPC and SMPS readings.

3.1. Preschool I

Fig. 1a shows the contour plot for October 30, 2019. This figure shows the production of a copious amount of small particles (smaller than 3 nm) throughout the day from 9:30 am to 3:30 pm suggesting the sustained presence of the precursors of the new particles. Fig. 1a also shows a significant increase in the particle number (PN) concentration for particles larger than 3 nm around 11:42 am attributed to the candle burning. However, the candle events did not dominate the measured total particle number concentration and particle mode diameter, suggesting that a different source rather than combustion (candle burning) was present throughout the day that produced a copious amount of small particles.

Figs. S5 and S6 present the total particle number concentration (from 1 nm to 1 μm, combined SMPS and CPC) and particle mode diameter (1–30 nm, only SMPS) with time, respectively, on October 30, 2019. The average total particle concentration and the average mode diameter were

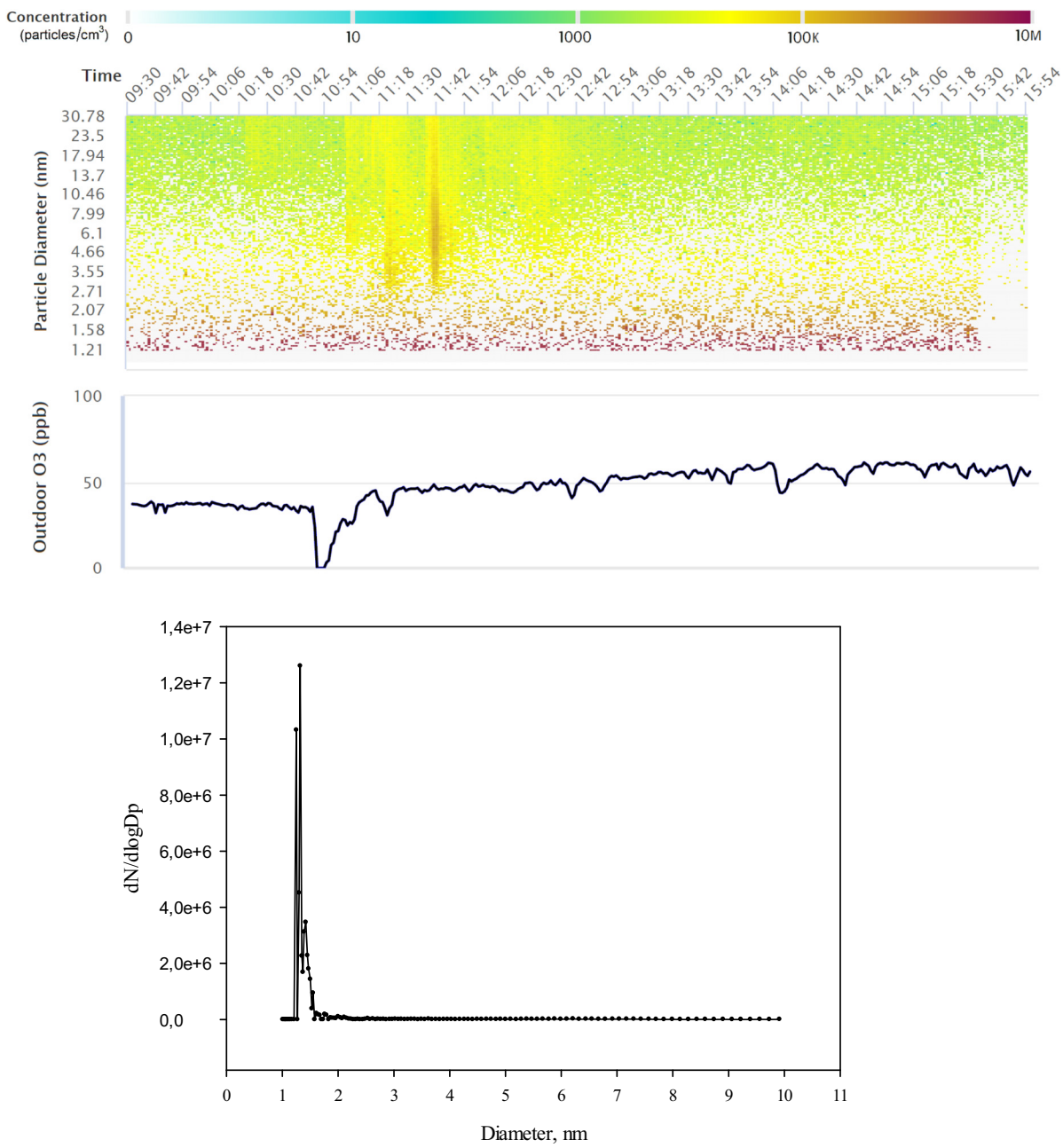

Fig. 1. The contour plot (Fig. 1a) and the ozone concentration (Fig. 1b) for the measurements conducted on October 30, 2019, and particle number size distribution (Fig. 1c) for October 30, 2019, 11:06 am–11:11 am time.

2.81 × 10^6 (SD 9.90 × 10^5) particles/cm^3 and 1.32 (SD 0.14) nm, respectively.

Fig. 1a demonstrates a continuous major CPF event in Preschool I as the average particle mode diameter was 1.32 (SD 0.14) nm. Significantly high concentrations of the sub-3 nm particles were observed such that the concentration of the new particles (1–3 nm) was on average 2.81 × 10^6 (SD 0.99 × 10^6) particles/cm^3. While most of the particles produced during candle burning were higher than 3 nm, particles between 2 and 3 nm were also observed during the candle event. Nucleation of particles larger than 3 nm in the order of 10^4 particles/cm^3 was also observed between 12 and 12:30 pm when the mentors microwaved the children's lunch. Fig. 1c shows a unimodal particle size distribution with a mode diameter to be at 1.32 nm. At that period, the CPF event was observed.

We also observed the continuous major CPF event on October 29, 2019 (the whole day) (Figs. 2a, S7, and S8). Two nucleation events due to candle burning events were observed at 11:53 am and 1:24 pm on October 29, 2019. On this day, the average particle number concentration and mode diameters were 1.11 × 10^6 (SD 1.83 × 10^6) particles/cm^3 and 1.41 (SD 0.33) nm, respectively. The morning candle burning was practiced every day during the candle game, while the occasional afternoon candle burning was because of the birthday celebration of the children. Fig. 2c shows a unimodal particle size distribution with a mode diameter to be at 1.25 nm.

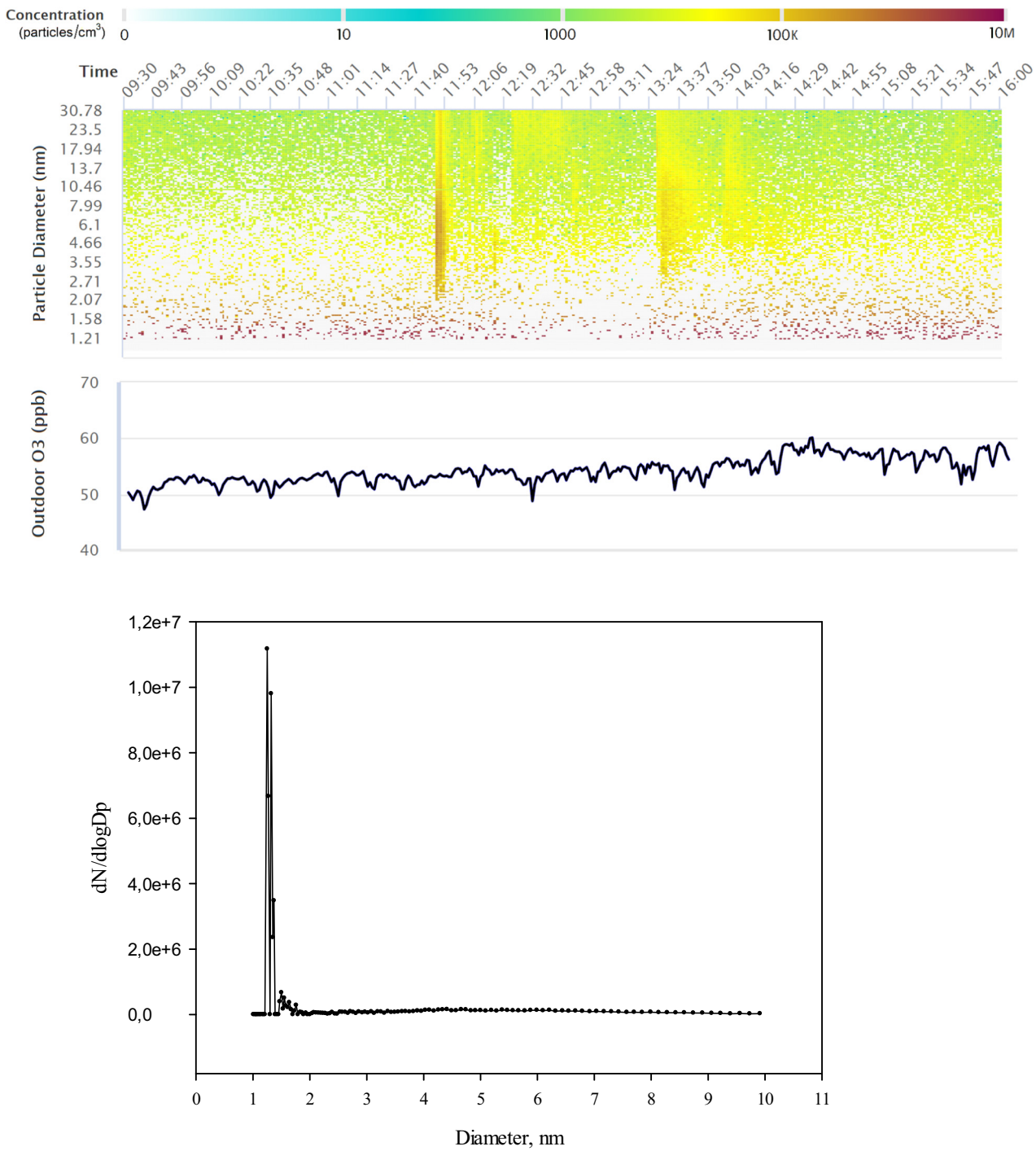

Fig. 2. The contour plot (a) and the ozone concentration (b) for the measurements conducted on October 29, 2019, and particle number distribution (c) for October 29, 2019, 11:47 am–11:52 am time.

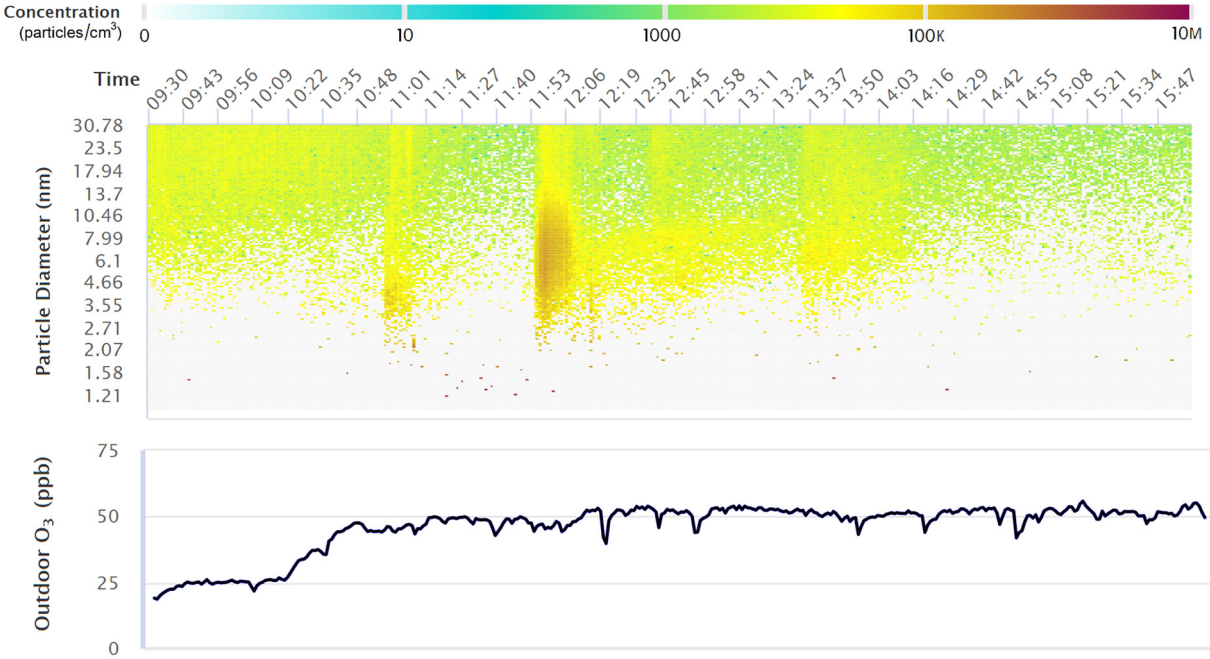

Fig. 3. The contour plot (a) and the ozone concentration (b) for the measurements conducted on October 31, 2019, 2019.

The CPF event became less visible and discontinued on October 31, 2019, as shown by Figs. 3a, S10, and S11 (the contour plot, variations of particle number concentration, and particle mode diameter with time, respectively). On this day, two nucleation events were observed at approximately 11 am, and 11:55 am, consistent with the previous days. Particles from the candle burning nucleated with the average mode diameter larger than 3 nm (on average 4.8 (SD 2.83) nm). However, particles down to 2 nm were observed consistent with the observations reported by Wallace et al. (Wallace et al., 2019). In this study, the particle mode diameter was 24 nm in the morning (Fig. S11) in the absence of any particular source.

Fig. 3a shows the production of a significant number of particles from the candle burning around 11:53 am that grew to larger sizes with time until 1 pm. However, the concentration of these particles decreased with time, creating a banana shape trend. This banana shape could be attributed to the coagulation of the candle particles with time, particularly from 12 to 1 pm, when no indoor activities were conducted. This particle growth with time coincided with decreases in particle number concentration. Similar observations were made for other days in this study such that a banana shape trend in particle diameter was observed for candle burning particles around noon (Figs. 1a and 2a).

The presence of secondary organic aerosol (SOA) in an indoor environment has been well explained (Weschler and Carslaw, 2018). Literature reports that usually, the diameter of such particles is less than 500 nm (Weschler and Carslaw, 2018). Very recently, Wu et al. (2019) observed new particle formation (NPF) events in an office and concluded that the major source of new particles was ozonolysis of monoterpenes in the office. To better understand if the new particles observed in this study are SOA, we studied the variations of outdoor ozone concentration during CPF and non-CPF events. We examined the outdoor ozone concentrations during several days of this study. Fig. 1a and b shows that CPF occurred throughout the day on October 30, 2019, when the ozone concentration was on average 47.27 (SD 11.13) ppb (below 50 ppb in the morning and also above 50 ppb in the afternoon). On October 29, 2019, the ozone concentration was relatively higher than the ozone concentration on October 30, 2019. It varied between 50 and 60 ppb during the day with an increasing trend from the morning to the afternoon. Again, CPF was observed the whole day on October 29, 2019, similar to October 30, 2019. However, the observed concentration of the particles was lower on October 29 compared to the October 30, 2019 (1.26×10^6 (SD 0.19×10^6) particles/cm^3) even the ozone concentration was higher (54.25 (SD 2.36) ppb on October 29, 2019, and 47.27 (SD 11.13) ppb on October 30, 2019). On October 31, 2019, when the ozone concentration increased to approximately 50 ppb, no CPF events were observed. The average total particle number concentration reduced to (2.8×10^4 (SD 1.01×10^4) particles/cm^3 (Fig. S10).

On November 1, 2019, in the afternoon (after 2 pm), compared to the morning, the particle concentration considerably increased while the mode diameter decreased, suggesting a reverse association between the particle number concentration and particle mode diameter (Figs. S12 and S13). In the morning, the mode diameter values were larger than 2 nm with an average value of 2.38 (SD 0.79) nm in diameter and 8.16×10^5 (SD 4.33×10^5) particles/cm^3, in concentration indicating the minor CPF events. However, after 2 pm, the concentration increased to (4.65×10^6 (SD 3.74×10^6)) particles/cm^{3,} and the average mode diameter decreased to 1.23 (SD 0.12) nm (Fig. 4c). While a major CPF event was observed only in the afternoon (Fig. 4a), an insignificant difference was observed between the morning (55.4 (SD 9.5) ppb) and the afternoon (57 (SD 8.79) ppb) ozone concentrations.

The findings in Preschool I shows that the major CPF occurred at outdoor ozone concentrations close to 50 ppb and higher. However, we observed cases, when the ozone concentration was higher than 50 ppb and no major CPF events, were found. Since no strong associations between CPF events and ozone concentrations within the studied range of the ozone concentration were observed, we concluded that another factor could control the major CPF events. Studies report that children's activities like painting, applications with glue, also spicy food can contribute to the SOA formation (Bhangar et al., 2011; Long et al., 2000b; Morawska et al., 2003; Wallace, 2006). Recent studies showed that SOA could be produced due to the reaction of indoor ozone and carbonyl and terpenes from cooking additives and condiments (Klein et al., 2019; Liu et al., 2017).

Measurements were performed over a weekend (November 16 and 17, 2019), when no children and indoor activities were present to examine the effect of indoor VOCs.

Figs. 5, S15, and S16 present the contour plot, total particle concentration, and mode diameter variations with time on Sunday, November 17, 2019, the weekend study I. The average particle number concentration was 1.2×10^4 (SD 4.6×10^4) particles/cm^3. The average mode diameter for that day was on average 7.8 (SD 4.8) nm. Certainly, no CPF event was registered for this day (Fig. 5a), although in the late afternoon, the ozone

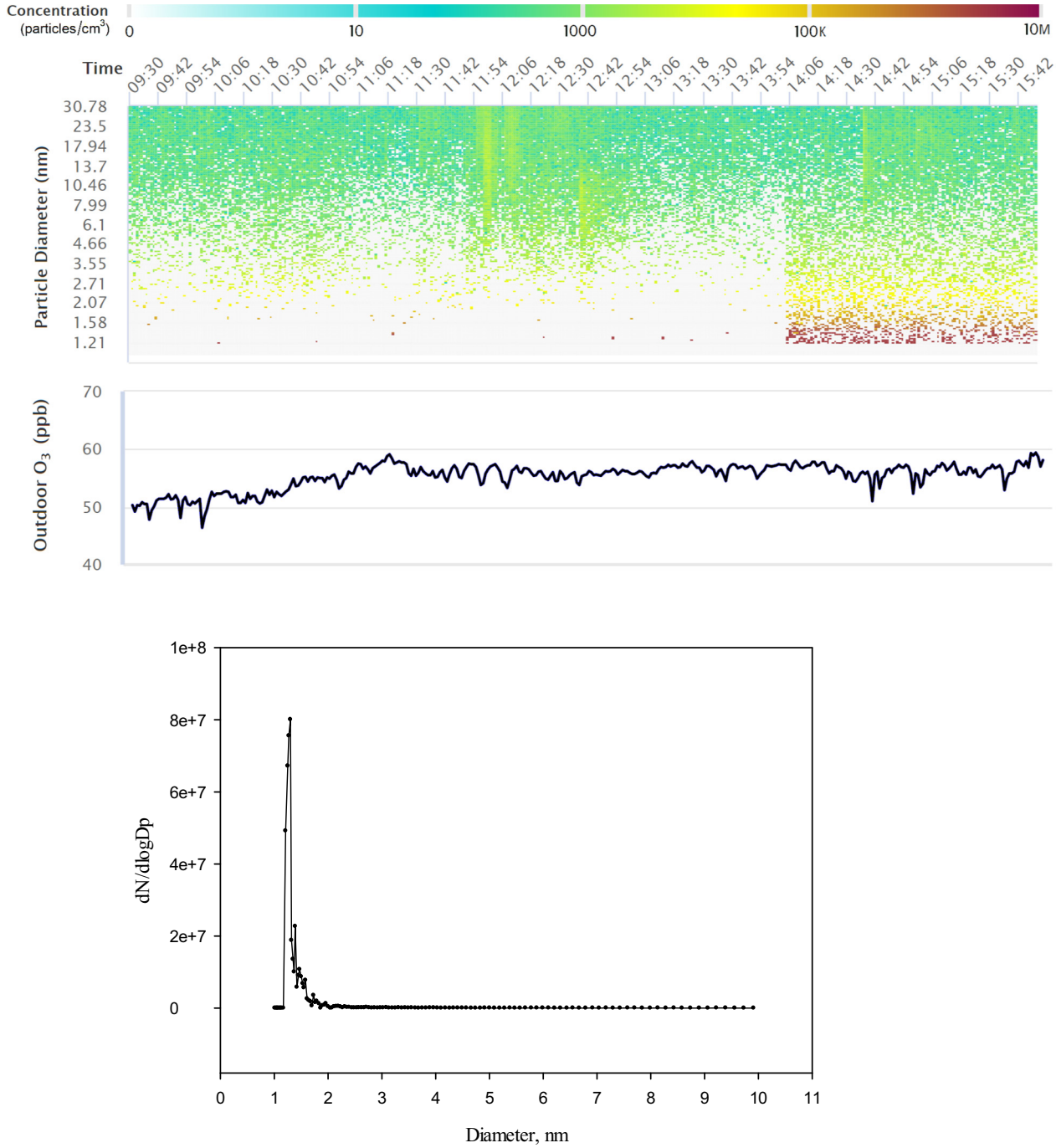

Fig. 4. The contour plot (Fig. 4a) and the ozone concentration (Fig. 4b) for the measurements conducted on November 1, 2019, and particle number distribution (Fig. 4c) for November 1, 2019, 2:36 pm–2:40 pm time.

concentration exceeded 50 ppb (Fig. 5b). A gradual increase in the particle diameter was observed over the time that could be due to the coagulation of the traffic particles with the mode diameter around 6 nm, formed early in the morning (before 10 am). Fig. 5a shows that in the morning before 10 am. The size of these particles increased to approximately 18 nm around 2:30 pm, creating a banana shape in Fig. 5a.

Figs. 6, S18, and S19 present the contour plot, total particle number concentration, and average mode diameter variations with time on Saturday, November 16, 2019, weekend study II. In the morning from 11 am to 12:30 pm, when the outdoor ozone concentration was below 50 ppb, the mode diameter of particles fluctuates between 6 and 30 nm, with the average mode diameter to be 14.42 nm. Nevertheless, when the outdoor ozone concentration increased after 12:30 pm, a sudden decrease in particle mode diameter was observed such that the particle mode diameter varied from 3 to 8 nm with an average value of 5 nm. The average particle concentration registered for this day was 1.71×10^5 (SD 2.14×10^5) particles/cm^3. Overall, no CPF event was observed during this weekend experiment.

Table 1 shows a comparison of particle mode diameter and total particle concentrations during major CPF events, normal (no CPF events) weekdays and weekends in Preschool I. Major CPF events included October 29, October 30, and November 1, 2019 (in the afternoon). November 1, 2019, in the morning, was considered as the minor CPF event. The normal day included October 31, 2019. For the weekends, the average of the observations on Saturday and Sunday was considered. The average particle number concentrations in the range of 1–3 nm, 1–10 nm and larger than 10 nm were found to be 1.90×10^6 (SD 6.43×10^6) particles/cm^3, 1.25×10^6 (SD

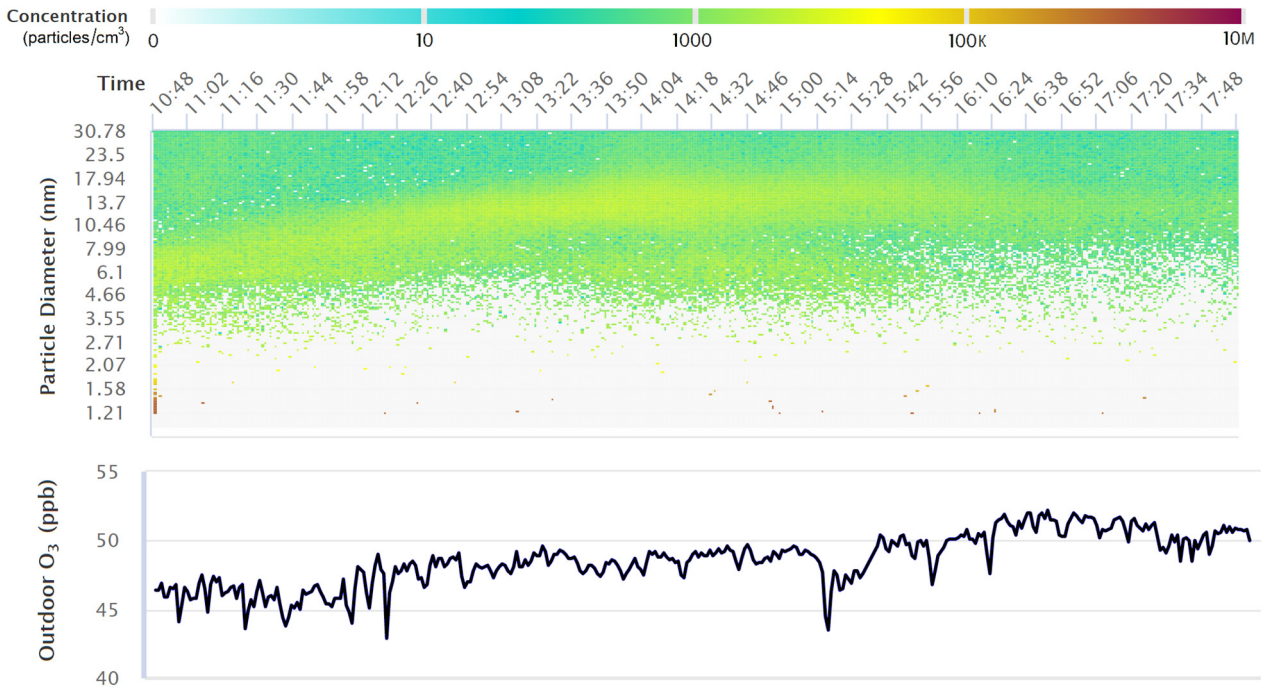

Fig. 5. The contour plot (Fig. 5a) and the ozone concentration (Fig. 5b) for the measurements conducted on November 17, 2019-Weekend study I.

9.20×10^5) particles/cm^3, and 2.13×10^3 (SD 1.74×10^3) particles/cm^3, respectively, suggesting that cluster mode particles predominated the particles in Preschool I. The average mode diameter during the CPF events was found to be 1.60 (SD 0.85) nm, while this value increased to 3.85 (SD 2.55) nm and 7.8 (SD 4.8) nm, during no CPF events and weekends (Fig. 6c), respectively. Table 1 also shows approximately 18 to 25 °C difference between the outdoor/indoor temperature that can create a pressure gradient for the penetration of outdoor ozone and particles to the indoor.

3.2. Preschool II

The results for Preschool II are presented in the supplementary materials.

4. Discussion

4.1. Emission rates

To provide a thorough comparison of the examined preschools, emission rate analyses were performed for the CPF events in both preschools. The average air exchange rate in Preschool I was 1.99×10^{-1} (SD 2.00×10^{-2}) min^{-1}, while for Preschool II, this value was on average twice lower 1.10×10^{-1} (SD 5.60×10^{-2}) min^{-1}. While the indoor/outdoor temperature difference was higher in Preschool II compared to Preschool I, the lack of windows limited the ventilation rate in Preschool II that led to the lower values of the air exchange rate. The emission rate was estimated for October 29 morning and afternoon, and October 30 in Preschool I, and for November 20 morning and afternoon and November 25 in Preschool II.

The estimated emission rate in Preschool I for 1 to 30 nm size particles was 9.57×10^6 (SD 1.92×10^6) particles/min. The emission rate value during the morning of October 29th was 3.41×10^7 particles/min which is higher than the value in the afternoon of the same day (1.47×10^{-6} particles/min) due to candle burning in the morning. In comparison, for Preschool II for the same size range, the results varied significantly from 2.60×10^3 to 2.16×10^7 particles/min and on average constituted 7.25×10^6 (SD 12.4×10^6) particles/min. The peak of 2.16×10^{-7} particles/min appeared on the morning of November 20th due to cleaning activities at this time. He et al. (2004) reported the emission rate for the sweeping floor to be 1.2×10^{10} particles/min, which is very close to our values for both preschools. According to Stabile et al. (2021), depending on the type of the cleaning product the emission factor ranged from 0 to approximately 2.4×10^{10} particles/min (1.1×10^{11} particles/m^2). The observed variability in the emission rate in Preschool II could be due to using different brands of cleaning products.

However, there are other two limitations contributing to reduced emission factor value. Firstly, the gas is not well-mixed in the room, so that the non-uniform distribution of particles in the environment could be a potential cause for such small values. Secondly, no coagulation is considered during the calculations of the emission rate.

4.2. Sources of the CPs

During the weekend studies in the two preschools, particles larger than 3 nm were observed (Figs. 5a, 6a, and S22), and thus, CPF events were eliminated. This observation suggests that major CPF events observed during the weekdays could be attributed to indoor sources except for smoking particles. We identified two classes of CPs, including primary CPs emitted directly from the sources such as candle burning and secondary CPs formed as a result of the oxidation of indoor VOCs or smoking VOCs by infiltrated ozone. The secondary CPs are likely to be SOA. Indoor VOCs were mainly emitted during cleaning activities with detergent solutions and painting, gluing, and using markers during the daily children's activities in the preschools. Infiltrated VOCs from smoking could also contribute to the SOA formation.

Our observations in the two preschools showed that no CPF events took place in the absence of the indoor activities, even at ambient ozone concentrations as high as 50 to 60 ppb. While No major CPF events were observed during indoor activities at ozone concentrations below 30 ppb. Despite the uncertainties in the frequency and intensity of CPF events, we concluded that indoor VOCs are the controlling factors in the CPF events.

We did observe an inconsistency in CPF events. For example, on October 31 and in the morning of November 1, we did not observe major CPF events (except minor CFPs from candle burning), although similar indoor activities would be expected to occur as the days with CPF events. On the other hand, on October 30 and 29, 2019, major CPF events occurred

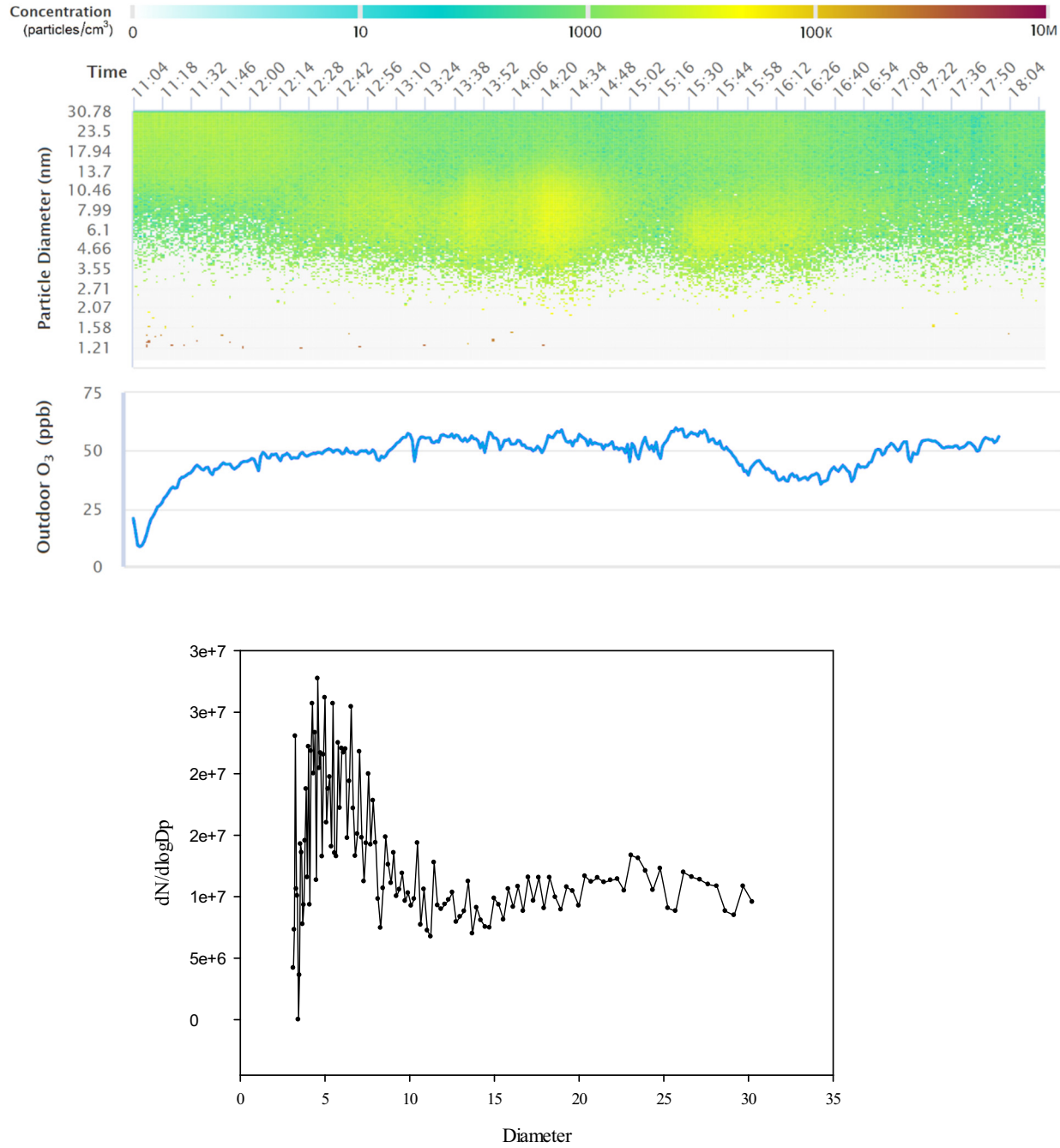

Fig. 6. The contour plot (a) and the ozone concentration (b) for the measurements conducted on November 16, 2019. Weekend study and particle number size distribution (c) for November 16, 2019, 3:25 pm–3:30 pm.

Table 1
A summary of particle mode diameter, number concentrations, outdoor ozone concentrations, and indoor/outdoor temperature for Preschool I.

Factor	Major CPF events*	Minor CPF events**	Normal days (no CPF)***	Weekend (no indoor activities)****
Average mode diameter (nm)	1.60 (SD 0.85)	2.38 (SD 0.79)	3.85 (SD 2.55)	7.8 (SD 4.8)
Average total particle concentration (particles/cm^3)	1.90×10^6 (SD 6.43×10^6)	8.16×10^5 (SD 4.33×10^5)	3.35×10^4 (SD 3.12×10^5)	1.71×10^5 (SD 2.14×10^5)
Outdoor ozone concentration (ppb)	52.10 (SD 7.98)	51.41 (SD 1.44)	46.26 (SD 9.25)	47 (SD 8.7)
Average outdoor temperature (°C)	9.61 (SD 4.80)	0.95 (SD 0.20)	9.80 (SD 2.58)	−3.06 (SD 1.52)
Average indoor temperature (°C)	25.49 (SD 2.05)	24.01 (SD 0.19)	23.17 (SD 0.42)	22.82 (SD 0.69)

* October 29, October 30, 2019, and November 1 afternoon, 2019 were taken as the major CPF events.
** November 1, 2019, in the morning was taken as the minor CPF event.
*** October 31, 2019, was taken as Normal days (no CPF).
**** November 16 and 17, 2019 were taken as weekends (no CPF).

throughout the day. This inconsistency could be due to the variability in VOC emissions from indoor activities, including painting, gluing, colored pencils for drawing, spicy food, and cleaning activities that did not occur daily at a precise schedule in Preschool I. According to the manager of Preschool I, in the morning from 9 am to 12 pm, students did painting and gluing based on their choice and interest. Thus, it was not practiced consistently for all children daily.

Major CPF events occurred more frequently in Preschool I compared to Preschool II such that the average PNC and mode diameter during the major CPF events in Preschool I were 1.90×10^6 (SD 6.43×10^6) particles/cm^3 and 1.60 (SD 0.85) nm, respectively, while these in Preschool II the average PNC and mode diameter during the major CPF events were found to be 3.61×10^8 (SD 3.15×10^8) and 3.25 (SD 3.58) nm respectively. The training program in Preschool I was children-driven. They could choose the tools to play based on their interest at any time. In the afternoon, occasionally, group paintings were conducted. Cleaning the toilets and sinks was done occasionally during the day with water and detergents. Major cleaning with detergents was practiced daily after 5 pm when the children left the facility, and thus, it was not captured in our study. In Preschool II, the activity program and their schedule were already assigned by the management and mentor team of the preschool. Thus, activities such as painting and gluing that contribute to indoor VOCs were practiced less frequently. This difference in the activity curriculum could impact the emissions of the particles and the exposure of the children to CPs.

Another factor that adds to the inconsistent CPF events refers to the type of the detergent that was used in the preschools. Stabile et al. (2021) recently tested 20 different brands of cleaning detergents in a chamber study and reported the resulting particle concentrations and emission factors down to 4 nm. Ten out of 20 detergents showed no production of particles. Similarly, Patel et al. (2020) found no CPF events down to 1 nm during several bleach mopping.

The effect of smoking on the formation of SOA has been well explained (Laursen et al., 2021). Literature reports that smoke from cigarettes can penetrate indoors and form SOA. However, no clear information exists if the SOA from smoking contributes to the CPF. A comparison between the UVPM concentration variations in preschool II (Figures in supplementary material) and the corresponding contour plots (Figures in supplementary material) show that the time at which peak concentration of UVPM was observed does not coincide with the time at which the major CPF events were observed. However, further investigation is required to understand the contribution of smoking to CPF events.

4.3. Minor CPF events

In this study, major CPFs took place over an extended time period while the minor CPF was observed discretely with time. Previous studies reported the presence of the sub-3 nm particles in even clean air (Laursen et al., 2021). The presence of the sub-3 nm particles indoors, particularly during the background measurements or the clean air in the laboratory, could be due to the traffic emissions that establish the background concentration (Rönkkö et al., 2017). However, this observation should be dominant mainly during the rush hours. If the sub-3 nm particles are observed through the day discreetly (minor CPF in the present study) other reasons than source emissions could be responsible for this observation. Patel et al. (Patel et al., 2020) concluded that the instrument may detect ions instead of particles smaller than 2 nm. A more plausible reason was proposed by Laursen et al. (Laursen et al., 2021) who concluded that uncertainties due to the loss corrections resulted in sharp concentration peaks (noises) at the lowest detection range (between 2 and 3 nm). They explained that when there exist a few particles at lower size limit sharp peaks in concentrations may appear due to the loss correction and can be considered as noises rather real existing particles (Laursen et al., 2021). However, the authors observed that if the emission of sub 3 nm particles in particular at the lowest detection limit is high such as candle burning particles then the noises may disappear.

5. Practical implications

For reducing children's exposure to CPs, it is recommended to replace candles with electronic candles and organic sources like markers, glue, or even spicy foods with other alternatives. The cleaning with detergents is recommended to be conducted before the children enter the preschools and after they leave the facility. Furthermore, the choice of the cleaning detergents is very important as a recent study showed that zero emissions can occur depending on the type of detergents (Stabile et al., 2021). Art activities such as gluing, painting, and drawing are suggested to be conducted in the seasons with a low ambient temperature that favors lower ozone productions and lower VOCs evaporations. The two factors promoting the ozone infiltration and specific to Nur-Sultan city of Kazakhstan was the relatively high wind speed and the prevailing westerly wind (on average 240 °C) towards the windows of the preschools, and also high-temperature difference between indoor and outdoor up to 40 °C creating a driving force for the ozone infiltration.

6. Limitations of this study

The emission rate values presented in this study should be considered as lower limit values as the particle coagulation rate has not been considered in the model.

In this study, gas concentrations, including indoor ozone and indoor VOCs, were not measured. Particularly, the data for indoor VOCs can help us to understand the SOA formation better.

No exposure assessment was done in this study. However, as future work exposure and dose assessment based on the particle surface area data obtained in this study will be conducted.

7. Conclusion

The formation of the cluster particles (1–3 nm) in preschools was demonstrated in this study. The CPF events were divided into major (concentrations higher than 10^6 particles/cm^3) and minor (concentrations lower than 10^6 particles/cm^3) events depending on the concentration of the sub-3 nm particles. We divide the cluster particles (CPs) in preschools into two categories, primary CPs and secondary CPs. Primary CPs are directly emitted from sources such as candle burning, and smoking while secondary CPs are likely to be SOA that result from the oxidation of the indoor VOCs generated from painting, markers, gluing, and more likely cleaning activities, by the infiltrated ambient ozone. We observed that both ambient ozone concentration and indoor activities generating VOCs matter for the CPF events, with indoor activities to be the controlling factor. We conclude that the activity curriculum of the preschools impacts the exposure of the children to the indoor particles, particularly CPs. A preschool designed to give more freedom of activities to the children is likely to have a higher level of CPs because of the random children's activities and arbitrary choices of playing. Opportunities exist to reduce the emissions of CPs in preschools.

CRediT authorship contribution statement

Mehdi Amouei Torkmahalleh: Supervision, Conceptualization, Validation, Methodology, Writing – review & editing. **Kamila Turganova:** Investigation, Data curation. **Zhuldyz Zhigulina:** Investigation, Data curation. **Tomiris Madiyarova:** Investigation, Data curation. **Enoch Kwasi Adotey:** Resources, Investigation. **Milad Malekipirbazari:** Formal analysis. **Giorgio Buonanno:** Writing – review & editing. **Luca Stabile:** Writing – review & editing.

Declaration of competing interest

The authors declare that they have no known competing financial interests or personal relationships that could have appeared to influence the work reported in this paper.

Acknowledgment

The authors of this study are the member of the Chemical and Aerosol Research Team (CART) and the Environment and Resource Efficiency Cluster (EREC). They would like to acknowledge CART and EREC for providing their supports to conduct this research. The authors of this study thanks Prof. Lidia Morawska, for reviewing the first draft of the manuscript that helped to improve it.

Appendix A. Supplementary data

Supplementary data to this article can be found online at https://doi.org/10.1016/j.scitotenv.2021.151756.

References

Oberdörster, G., Sharp, Z., Atudorei, V., Elder, A., Gelein, R., Kreyling, W., Cox, C., 2004. Translocation of inhaled ultrafine particles to the brain. Inhal. Toxicol. 16 (6–7), 437–445.

Slezakova, K., de Oliveira Fernandes, E., do Carmo Pereira, M., 2019. Assessment of ultrafine particles in primary schools: emphasis on different indoor microenvironments. Environ. Pollut. 246, 885–895.

Rim, D., Gall, E.T., Kim, J.B., Bae, G.-N., 2017. Particulate matter in urban nursery schools: a case study of Seoul, Korea during winter months. Build. Environ. 119, 1–10.

Naseri, M., Jouzizadeh, M., Tabesh, M., Malekipirbazari, M., Gabdrashova, R., Nurzhan, S., Farrokhi, H., Khanbabaie, R., Mehri-Dehnavi, H., Bekezhankyzy, Z., 2019. The impact of frying aerosol on human brain activity. Neurotoxicology 74, 149–161.

Fonseca, J., Slezakova, K., Morais, S., Pereira, M., 2014. Assessment of ultrafine particles in Portuguese preschools: levels and exposure doses. Indoor Air 24 (6), 618–628.

Morawska, L., Ristovski, Z., Jayaratne, E., Keogh, D.U., Ling, X., 2008. Ambient nano and ultrafine particles from motor vehicle emissions: characteristics, ambient processing and implications on human exposure. Atmos. Environ. 42 (35), 8113–8138.

Morawska, L., Ayoko, G., Bae, G., Buonanno, G., Chao, C., Clifford, S., Fu, S.C., Hänninen, O., He, C., Isaxon, C., 2017. Airborne particles in indoor environment of homes, schools, offices and aged care facilities: the main routes of exposure. Environ. Int. 108, 75–83.

Sarwar, G., Corsi, R., Allen, D., Weschler, C., 2003. The significance of secondary organic aerosol formation and growth in buildings: experimental and computational evidence. Atmos. Environ. 37 (9–10), 1365–1381.

Oliveira, M., Slezakova, K., Delerue-Matos, C., Pereira, M.d.C., Morais, S., 2017. Indoor air quality in preschools (3-to 5-year-old children) in the Northeast of Portugal during spring–summer season: pollutants and comfort parameters. J. Toxicol. Environ. Health A 80 (13-15), 740–755.

Gaspar, F., Maddalena, R., Williams, J., Castorina, R., Wang, Z.M., Kumagai, K., McKone, T., Bradman, A., 2018. Ultrafine, fine, and black carbon particle concentrations in California child-care facilities. Indoor Air 28 (1), 102–111.

Daisey, J.M., Angell, W.J., Apte, M.G., 2003. Indoor air quality, ventilation and health symptoms in schools: an analysis of existing information. Indoor Air 13 (LBNL-48287).

Ramachandran, G., Adgate, J.L., Banerjee, S., Church, T.R., Jones, D., Fredrickson, A., Sexton, K., 2005. Indoor air quality in two urban elementary schools—measurements of airborne fungi, carpet allergens, CO2, temperature, and relative humidity. J. Occup. Environ. Hyg. 2 (11), 553–566.

Godwin, C., Batterman, S., 2007. Indoor Air Quality in Michigan Schools.

Chithra, V.S., Nagendra, S.M.S., 2012. Indoor air quality investigations in a naturally ventilated school building located close to an urban roadway in Chennai, India. Build. Environ. 54, 159–167.

Yang, W., Sohn, J., Kim, J., Son, B., Park, J., 2009. Indoor air quality investigation according to age of the school buildings in Korea. J. Environ. Manag. 90 (1), 348–354.

Pegas, P.N., Evtyugina, M.G., Alves, C.A., Nunes, T., Cerqueira, M., Franchi, M., Pio, C., Almeida, S.M., Freitas, M.do C., 2010. Outdoor/indoor air quality in primary schools in Lisbon: a preliminary study. Quim. Nova 33, 1145–1149.

Kotzias, D., 2005. Indoor air and human exposure assessment-needs and approaches. Exp. Toxicol. Pathol. 57, 5–7.

Sofuoglu, S.C., Aslan, G., Inal, F., Sofuoglu, A., 2011. An assessment of indoor air concentrations and health risks of volatile organic compounds in three primary schools. Int. J. Hyg. Environ. Health 214 (1), 36–46.

Amouei Torkmahalleh, M., Zhigulina, Z., Madiyarova, T., Turganova, K., Adotey, E.K., Sabanov, S., 2021. Exposure to fine, ultrafine particles and black carbon in two preschools in Nur-Sultan City of Kazakhstan. Indoor Air 31 (4), 1178–1186. https://doi.org/10.1111/ina.12799.

Morawska, L., Ayoko, G.A., Bae, G.N., Buonanno, G., Chao, C.Y.H., Clifford, S., Fu, S.C., Hänninen, O., He, C., Isaxon, C., 2017. Airborne particles in indoor environment of homes, schools, offices and aged care facilities: the main routes of exposure. Environ. Int. 108, 75–83.

Błaszczyk, E., Rogula-Kozłowska, W., Klejnowski, K., Kubiesa, P., Fulara, I., Mielżyńska-Švach, D., 2017. Indoor air quality in urban and rural kindergartens: short-term studies in Silesia, Poland. Air Qual. Atmos. Heal. 10 (10), 1207–1220.

Weschler, C.J., Shields, H.C., 1999. Indoor ozone/terpene reactions as a source of indoor particles. Atmos. Environ. 33 (15), 2301–2312. https://doi.org/10.1016/S1352-2310(99)00083-7.

Bahreini, R., Keywood, M.D., Ng, N.L., Varutbangkul, V., Gao, S., Flagan, R.C., Seinfeld, J.H., Worsnop, D.R., Jimenez, J.L., 2005. Measurements of secondary organic aerosol from oxidation of cycloalkenes, terpenes, and m-xylene using an aerodyne aerosol mass spectrometer. Environ. Sci. Technol. 39 (15), 5674–5688.

Chen, X., Hopke, P.K., 2010. A chamber study of secondary organic aerosol formation by limonene ozonolysis. Indoor Air 20 (4), 320–328.

Sarwar, G., Corsi, R., Allen, D., Weschler, C., 2003. The significance of secondary organic aerosol formation and growth in buildings: experimental and computational evidence. Atmos. Environ. 37 (9–10), 1365–1381.

Waring, M.S., Wells, J.R., Siegel, J.A., 2011. Secondary organic aerosol formation from ozone reactions with single terpenoids and terpenoid mixtures. Atmos. Environ. 45 (25), 4235–4242.

Coleman, B.K., Lunden, M.M., Destaillats, H., Nazaroff, W.W., 2008. Secondary organic aerosol from ozone-initiated reactions with terpene-rich household products. Atmos. Environ. 42 (35), 8234–8245.

Destaillats, H., Lunden, M.M., Singer, B.C., Coleman, B.K., Hodgson, A.T., Weschler, C.J., Nazaroff, W.W., 2006. Indoor secondary pollutants from household product emissions in the presence of ozone: a bench-scale chamber study. Environ. Sci. Technol. 40 (14), 4421–4428.

Donahue, N.M., Tischuk, J.E., Marquis, B.J., Hartz, K.E.H., 2007. Secondary organic aerosol from limona ketone: insights into terpene ozonolysis via synthesis of key intermediates. Phys. Chem. Chem. Phys. 9 (23), 2991–2998.

Fadeyi, M.O., Weschler, C.J., Tham, K.W., Wu, W.Y., Sultan, Z.M., 2013. Impact of human presence on secondary organic aerosols derived from ozone-initiated chemistry in a simulated office environment. Environ. Sci. Technol. 47 (8), 3933–3941.

Leungsakul, S., Jaoui, M., Kamens, R.M., 2005. Kinetic mechanism for predicting secondary organic aerosol formation from the reaction of D-limonene with ozone. Environ. Sci. Technol. 39 (24), 9583–9594.

Librando, V., Tringali, G., 2005. Atmospheric fate of OH initiated oxidation of terpenes. Reaction mechanism of α-pinene degradation and secondary organic aerosol formation. J. Environ. Manag. 75 (3), 275–282.

Presto, A.A., Huff Hartz, K.E., Donahue, N.M., 2005. Secondary organic aerosol production from terpene ozonolysis. 1. Effect of UV radiation. Environ. Sci. Technol. 39 (18), 7036–7045.

Sarwar, G., Corsi, R., 2007. The effects of ozone/limonene reactions on indoor secondary organic aerosols. Atmos. Environ. 41 (5), 959–973.

Waring, M.S., Siegel, J.A., 2013. Indoor secondary organic aerosol formation initiated from reactions between ozone and surface-sorbed d-limonene. Environ. Sci. Technol. 47 (12), 6341–6348.

Walser, M.L., Park, J., Gomez, A.L., Russell, A.R., Nizkorodov, S.A., 2007. Photochemical aging of secondary organic aerosol particles generated from the oxidation of D-limonene. J. Phys. Chem. A 111 (10), 1907–1913.

Rohr, A.C., 2013. The health significance of gas-and particle-phase terpene oxidation products: a review. Environ. Int. 60, 145–162.

Kephalopoulos, S., Kotzias, D., Koistinen, K., 2007. European collaborative action, urban air, indoor environment and human exposure. Impact of Ozone-Initiated Terpene Chemistry on Indoor Air Quality and Human Health Report.

Morawska, L., He, C., Johnson, G., Guo, H., Uhde, E., Ayoko, G., 2009. Ultrafine particles in indoor air of a school: possible role of secondary organic aerosols. Environ. Sci. Technol. 43 (24), 9103–9109.

Stabile, L., De Luca, G., Pacitto, A., Morawska, L., Avino, P., Buonanno, G., 2021. Ultrafine particle emission from floor cleaning products. Indoor Air 31 (1), 63–73.

Bhangar, S., Adams, R.I., Pasut, W., Huffman, J., Arens, E.A., Taylor, J.W., Bruns, T.D., Nazaroff, W.W., 2016. Chamber bioaerosol study: human emissions of size-resolved fluorescent biological aerosol particles. Indoor Air 26 (2), 193–206.

Mullen, N., Bhangar, S., Hering, S., Kreisberg, N., Nazaroff, W., 2011. Ultrafine particle concentrations and exposures in six elementary school classrooms in northern California. Indoor Air 21 (1), 77–87.

Wallace, L., Jeong, S.G., Rim, D., 2019. Dynamic behavior of indoor ultrafine particles (2.3-64 nm) due to burning candles in a residence. Indoor Air 29 (6), 1018–1027.

Pedata, P., Malorni, L., Sannolo, N., Conturso, M., Scantone, S., Sirignano, M., Ciajolo, A., Anna, A., 2016. Characterization and inflammatory potential of sub-10nm particles from gas cooking appliances. Chem. Eng. Trans. 47, 433–438.

Patel, S., Sankhyan, S., Boedicker, E.K., DeCarlo, P.F., Farmer, D.K., Goldstein, A.H., Katz, E.F., Nazaroff, W.W., Tian, Y., Vanhanen, J., 2020. Indoor particulate matter during HOMEChem: concentrations, size distributions, and exposures. Environ. Sci. Technol. 54 (12), 7107–7116.

Wu, T., Stevens, P., Huber, H., Tasoglou, A., Boor, B., 2019. Indoor measurements of nanocluster aerosols and new particle formation. AAAR 37th Annual Conference Abstracts, Portland, USA.

Yao, L., Garmash, O., Bianchi, F., Zheng, J., Yan, C., Kontkanen, J., Junninen, H., Mazon, S.B., Ehn, M., Paasonen, P., 2018. Atmospheric new particle formation from sulfuric acid and amines in a Chinese megacity. Science 361 (6399), 278–281.

Ahonen, L., Kangasluoma, J., Lammi, J., Lehtipalo, K., Hämeri, K., Petäjä, T., Kulmala, M., 2017. First measurements of the number size distribution of 1–2 nm aerosol particles released from manufacturing processes in a cleanroom environment. Aerosol Sci. Technol. 51 (6), 685–693.

Vanhanen, J., Miettinen, E., Chen, L., Väkevä, M., 2016. Indoor Air Measurements of 1-4 nm Particle Number Size Distribution Using Nano Condensation Nucleus Counter.

Amouei Torkmahalleh, M., Ospanova, S., Baibatyrova, A., Nurbay, S., Zhanakhmet, G., Shah, D., 2018. Contributions of burner, pan, meat and salt to PM emission during grilling. Environ. Res. 164, 11–17.

Wallace, L.A., Emmerich, S.J., Howard-Reed, C., 2004. Source strengths of ultrafine and fine particles due to cooking with a gas stove. Environ. Scie. Technol. 38 (8), 2304–2311.

Weschler, C.J., Carslaw, N., 2018. Indoor chemistry. ACS Publications.

Bhangar, S., Mullen, N., Hering, S., Kreisberg, N., Nazaroff, W., 2011. Ultrafine particle concentrations and exposures in seven residences in northern California. Indoor Air 21 (2), 132–144.

Long, C.M., Suh, H.H., Koutrakis, P., 2000. Characterization of indoor particle sources using continuous mass and size monitors. J. Air Waste Manag. Assoc. 50 (7), 1236–1250.

Morawska, L., He, C., Hitchins, J., Mengersen, K., Gilbert, D., 2003. Characteristics of particle number and mass concentrations in residential houses in Brisbane, Australia. Atmos. Environ. 37 (30), 4195–4203.

Wallace, L., 2006. Indoor sources of ultrafine and accumulation mode particles: size distributions, size-resolved concentrations, and source strengths. Aerosol Sci. Technol. 40 (5), 348–360.

Klein, F., Baltensperger, U., Prévôt, A.S., El Haddad, I., 2019. Quantification of the impact of cooking processes on indoor concentrations of volatile organic species and primary and secondary organic aerosols. Indoor Air 29 (6), 926–942.

Liu, T., Liu, Q., Li, Z., Huo, L., Chan, M., Li, X., Zhou, Z., Chan, C.K., 2017. Emission of volatile organic compounds and production of secondary organic aerosol from stir-frying spices. Sci. Total Environ. 599, 1614–1621.

He, C., Morawska, L., Hitchins, J., Gilbert, D., 2004. Contribution from indoor sources to particle number and mass concentrations in residential houses. Atmos. Environ. 38 (21), 3405–3415.

Laursen, Rasmussen, Rosati, Gutzke, Østergaard, Ravn, Kjærgaard, Bilde, Glasius, Sigsgaard, Torben, 2021. … See fewer authors First published: 07 July 2021. Indoor Air https://doi.org/10.1111/ina.12902 Acute health effects from exposure to indoor ultrafine particles—a randomized controlled crossover study among young mild asthmatics.

Rönkkö, T., Kuuluvainen, H., Karjalainen, P., Keskinen, J., Hillamo, R., Niemi, J.V., Saukko, E., 2017. Traffic is a major source of atmospheric nanocluster aerosol. Proc. Natl. Acad. Sci. 114 (29), 7549–7554.